

Production of double hypernuclei with high energy antiprotons at PANDA

Michelangelo Agnello,^{1,2,*} Fabrizio Ferro,^{1,†} and Felice Iazzi^{1,2,‡}

¹*Dipartimento di Fisica, Politecnico di Torino, I-10129 Torino, Italy*

²*INFN - Sezione di Torino, I-10125 Torino, Italy*

(Dated: 23rd November 2018)

The data available in literature, concerning the binding energy of double hypernuclei and their production techniques are briefly reviewed. Then, a new technique for producing double hypernuclei with antiprotons in flight and measuring their binding energy, proposed for the PANDA experiment at GSI, is investigated. Furthermore, preliminary results of the calculations for evaluating the double hypernuclei production and detection rates at the antiproton beam intensity foreseen at HESR are reported.

1. INTRODUCTION

The search for Double Hypernuclei (DH) (nuclei with two Λ 's replacing two non-strange nucleons), started in the sixties with the pioneering works of Danysz *et al.* and Prowse *et al.*, who first observed ${}_{\Lambda\Lambda}^{10}\text{Be}$ [1] and ${}_{\Lambda\Lambda}^6\text{He}$ [2] in emulsions exposed to K^- beams. Both experiments measured $B_{\Lambda\Lambda}({}_{\Lambda\Lambda}^AZ) = B_{\Lambda}({}_{\Lambda\Lambda}^AZ) + B_{\Lambda}({}_{\Lambda}^{A-1}Z)$ and $\Delta B_{\Lambda\Lambda}({}_{\Lambda\Lambda}^AZ) = B_{\Lambda}({}_{\Lambda\Lambda}^AZ) - B_{\Lambda}({}_{\Lambda}^{A-1}Z)$. The measurement of these quantities is at present the only experimental way to collect information about the Λ - Λ interaction and this is the reason of the stronger interest for the DH investigation with respect to single hypernuclei.

Other interesting features of DH are: a) their nuclear structure, with two levels both filled by strange hadrons; b) the possibility to explore the existence of the H dibaryon (a double strange system of 6 quarks predicted several years ago by Jaffe [3]); c) the information about the levels of the Ξ^- -atom, that is formed during the DH production process. In spite of the interest of these topics, only few experiments have been devoted to DH so far, mainly because of the difficulty to produce them. The traditional way is to produce a double strange Ξ^- particle via the strangeness exchange reaction $K^-(p, \Xi^-)K^+$ between a K^- meson and a proton bound in a nucleus, giving K^+ and Ξ^- ; this last, if decelerated to rest before decaying, can be captured inside a nucleus in which it interacts with a proton eventually releasing two Λ 's in two hypernuclear levels. The Ξ^- energy may be of order of some hundred MeVs, thus the slowing down process takes long time in ordinary matter. This explains why the probability of DH formation is so low: in fact, Danysz [1] and Prowse [2] observed one DH event each, among a K^- number of around a million.

In more recent experiments at BNL-AGS (E885) and KEK (PS E176) about $2 \cdot 10^4$ and 800 stopped Ξ^- 's respectively were observed, as reviewed by Pochodzalla [4].

Also at the planned Japanese Hadron Facility (JHF) the number of produced Ξ^- 's is expected to be of order of some thousands.

Furthermore the results obtained from experiments in terms of the above mentioned binding energies are too much different, clearly outside the experimental errors (see again [4]). Thus, while the existence of DH seems ascertained, an increase of statistics in the Ξ^- production is mandatory in order to step forward in their understanding.

Even though the traditional double strangeness exchange reaction will be pursued in the next future at JHF, as already mentioned, nevertheless the advent of new antiproton facilities, like HESR and JHF (second phase), allows the scientific community to explore alternative techniques of Ξ^- production from antiproton beams. A first one was proposed by Kilian [5] who suggested the annihilation of antiprotons at rest to produce K^- 's which subsequently could exchange strangeness with the residual nucleus, giving a Ξ^- hyperon. This technique requires a low energy antiproton machine and could be implemented, for instance, at CERN-AD.

But also in high energy antiproton machines like HESR and JHF, the Ξ^- hyperon may be directly produced in the antiproton annihilation reaction together with its antiparticle. The advantages are:

1. an higher rate with respect to the double reaction involving the annihilation at rest;
2. the presence of the antiparticle, to be used for tagging purposes.

The only disadvantage is the high momentum of the Ξ^- 's which need to be strongly decelerated before being captured at rest.

In this work we present the first preliminary results of a Monte Carlo simulation based on a simplified Intra-Nuclear Cascade Model, and performed to explore the rates of the produced and stopped Ξ^- 's and their probability to be captured forming a DH, as may be expected in the future PANDA experiment at the HESR-GSI facility.

*Electronic address: michelangelo.agnello@polito.it

†Electronic address: fabrizio.ferro@polito.it

‡Electronic address: felice.iazzi@polito.it

In sec. 2, the Ξ^- production techniques are illustrated; in sec. 3, the details of the antiproton annihilation into the Ξ^- 's are discussed; in sec. 4, the slowing down processes of Ξ^- inside the residual nucleus, in the target and in a second target devoted to the DH formation are analysed; in sec. 5, the results of our simulation in terms of DH rates are reported, and finally in sec. 6 the conclusions are drawn.

2. DOUBLE HYPERNUCLEI PRODUCTION WITH ANTIPROTONS

The simplest way for producing double strange nuclear systems is the DH direct formation through K^-K^+ reactions; on the contrary, an indirect method is the formation using Ξ^- capture at rest. The latter is known to have a higher rate [6].

A classical technique, adopted in the E176 experiment at KEK [7, 8], is based on a K^- kaon beam that induces the quasi-free nuclear reaction $K^- + p \rightarrow K^+ + \Xi^-$, thus producing a relatively high number of fast Ξ^- hyperons. These hyperons subsequently slow down in an emulsion stack and some $S = -2$ hypernuclei are formed following the Ξ^- capture at rest. In such kind of experiments, the emulsion is also the detector, with high enough resolution for tracking the formed hypernuclei and the products of their decay as well. A further improvement has been obtained in E373 at KEK [6], through a K^- beam (with momentum ~ 1.66 GeV/c) impinging on a diamond target in which the same reaction previously sketched occurs, though at far higher rate: in the experimental setup, the diamond block was followed by an emulsion stack as for E176 and the tracking detector was a fiber-bundle system. In all these experiments, the Ξ^- hyperon is captured in a light nucleus (i.e. carbon, nitrogen or oxygen) of the emulsion and therefore the observed double hypernuclei are ${}_{\Lambda\Lambda}^6\text{He}$, ${}_{\Lambda\Lambda}^{10}\text{Be}$ and ${}_{\Lambda\Lambda}^{13}\text{B}$.

Let us consider now the new technique proposed for the planned PANDA experiment at HESR-GSI; it relies on the same method of stopped Ξ^- 's, the main difference being that the hyperon production reaction is realized through an intense beam of antiprotons on a target of ${}^A\text{X}_Z^N$ nuclei (where A is the mass number, Z is the atomic number and N is the neutron number). The two reactions of interest are

$$\bar{p} + {}^A\text{X}_Z^N \rightarrow \bar{\Xi}^0 + \Xi^- + {}^{A-1}\text{X}_Z^{N-1} + \text{mesons}, \quad (1)$$

and

$$\bar{p} + {}^A\text{X}_Z^N \rightarrow \bar{\Xi}^+ + \Xi^- + {}^{A-1}\text{X}'_{Z-1}{}^N + \text{mesons}. \quad (2)$$

In reaction 1, the energetic antiproton annihilates on a neutron bound inside the X nucleus, while in reaction 2 it annihilates on a proton.

The fast Ξ^- slightly slows down in the production target itself, but the main part of its energy-loss process

occurs in a second separate target, that is also the place in which a statistical collection of double hypernuclei is supposed to be formed with some probability. In both reactions 1 and 2, beside the $S = -2$ hyperon Ξ^- , an anti-hyperon ($\bar{\Xi}^0$ or $\bar{\Xi}^+$) is released too, according to the strangeness and baryon conservation laws of strong interactions: this antiparticle can play a crucial role in the experimental detection of the whole double hypernuclei formation, as it may be used for trigger purposes.

Before proceeding, we want to point out that a still different technique has also been proposed [5], in which an antiproton interacts at rest with the ${}^A\text{X}_Z^N$ nucleus. A possible reaction is

$$\bar{p} + {}^A\text{X}_Z^N \rightarrow K^{*-} + K^0 + {}^{A-1}\text{X}_Z^{N-1} + \text{mesons}, \quad (3)$$

where K^{*-} is the K^- resonance at 892 MeV, that subsequently interacts with the residual nucleus, giving

$$K^{*-} + {}^{A-1}\text{X}_Z^{N-1} \rightarrow \Xi^- + K^0 + {}^{A-2}\text{X}_Z^{N-2} + \text{mesons}, \quad (4)$$

where the Ξ^- hyperon emerges with a momentum between 250 and 800 MeV/c approximately. In comparison with the method based on reactions 1 and 2, this technique has the disadvantage that the Ξ^- production occurs in two distinct steps (reactions 3 and 4), each one characterized by a somewhat low probability.

3. Ξ^- PRODUCTION

Let us start considering the Ξ^- production from reaction 1. A highly energetic antiproton \bar{p} interacts with a neutron n bound in a nuclear potential well. In what follows, we assume that the neutron be free; indeed, we expect that the total antiproton energy be of order of a few GeVs, while the average binding energy of a nucleon is roughly 8.8 MeV for the most tightly bound nuclei (i.e. ${}^{56}\text{Fe}$, ${}^{58}\text{Fe}$ and ${}^{62}\text{Ni}$).

If we consider \bar{p} momenta below π production threshold, the previous discussion allows us to consider the reaction as a two-body process, with the manifest advantage that its simple kinematics can be treated analytically, starting from the relativistic four-vector energy-momentum conservation; a similar discussion also applies to reaction 2. Hence, the two reactions simplify as

$$\bar{p} + n \rightarrow \bar{\Xi}^0 + \Xi^-, \quad (5)$$

and

$$\bar{p} + p \rightarrow \bar{\Xi}^+ + \Xi^-, \quad (6)$$

and from now on, we shall refer to them both as Strangeness Creation Reactions, namely SCRs.

The calculated threshold for the two SCRs (neglecting the slight difference between the proton mass and the neutron mass) is located at an antiproton momentum of

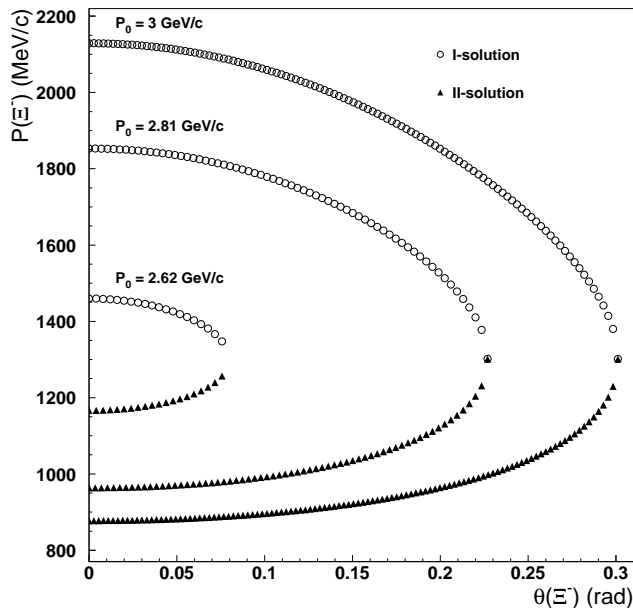


Figure 1: Plot of the hyperon momentum $P(\Xi^-)$ against the exit angle $\theta(\Xi^-)$ after SCR, considering three different values of the antiproton momentum, namely $P_0 = P_\pi^{\text{thr}} = 2.62$ GeV/c, $P_0 = 2.81$ GeV/c and $P_0 = P_\pi^{\text{thr}} = 3$ GeV/c. Both first and second kinematical solution are shown together. The curve labelled $P_0 = 3$ GeV/c has been adopted in our calculations.

$P^{\text{thr}} = 2.62$ GeV/c. Furthermore, the upper limit for the two-body exit channel (i.e. below pion production) is $P_\pi^{\text{thr}} = 3$ GeV/c.

Let be $\theta(\Xi^-)$ the angle between the direction of the incident antiproton \bar{p} and the direction of the outgoing Ξ^- hyperon, in the laboratory frame of reference. As it is well known from the relativistic kinematics of two-body reactions with threshold, the $\theta(\Xi^-)$ angle ranges between 0 and a maximum, θ_{max} , that is a function of the antiproton momentum P_0 . Furthermore, for any given value of $\theta(\Xi^-)$, two different momenta of the Ξ^- hyperon are allowed, whose relative probability strongly depends on the dynamics of the reaction itself. All these peculiar characteristics are shown in fig. 1 referring to the SCR of eq. 5: the dependence of the maximum angle θ_{max} on P_0 looks evident. At the antiproton momentum $P_0 = 3$ GeV/c, we obtain that the maximum angle is $\theta_{\text{max}} = 0.3$ rad.

The argument that led us to the choice of P_0 relies on the results of the quark-gluon string model [9] which predicts that the $\bar{p} + p \rightarrow \Xi^+ + \Xi^-$ reaction cross section σ shows a maximum at an antiproton momentum of around 3 GeV/c; in this case, the estimated maximum value is $\sigma_{\text{SCR}} \sim 2 \mu\text{b}$. Then, in our following calculations, we adopt $P_0 = 3$ GeV/c and we suppose that the same total nuclear cross section, $\sigma_{\text{SCR}} = 2 \mu\text{b}$, does hold

for both SCRs of eqs. 5 and 6. Lying on these physical hypotheses we obtain that, as far as the first (most probable) kinematical solution is concerned, the Ξ^- momentum ranges from 2129 MeV/c in the forward direction, to 1301 MeV/c at the limit angle while, considering the second solution, it spans from 877 MeV/c to about 1301 MeV/c respectively, as it can be seen in fig. 1.

Because of the high average momentum, the energy-loss process is of central importance in the planned experiment, and therefore the evaluation of the Ξ^- slowing down is worth while; we have performed it through a Monte Carlo simulation, as described in sec. 4. As a starting point, we generate $2 \cdot 10^5$ Ξ^- particles produced from SCR for each solution, assuming that reaction 5 occurs through a S-wave in the centre of mass frame of reference, namely assuming a uniform spherical distribution. According to the 3 GeV/c curve in fig. 1, the momentum spectra of the simulated Ξ^- hyperons are presented in fig. 2, for both kinematical solutions.

For tagging purposes, the momentum spectrum of the anti-hyperon is of great interest; our computer simulated results are reported in fig. 3. The Ξ^0 (or Ξ^+) momentum ranges from 871 MeV/c to 1798 MeV/c, with an average emission angle of 0.262 rad, in first solution, and from 1799 MeV/c to 2122 MeV/c in second solution, with an average angle equal to 0.125 rad. Furthermore, the maximum angle is 0.3 rad; therefore, the tagged anti-hyperon is expected to be released very close to the antiproton beam direction.

4. Ξ^- SLOWING DOWN

Let us start by noticing that the Ξ^- slowing down process consists of two distinct steps:

1. a sequence of nuclear elastic scattering events with some of the $A - 1$ nucleons of the residual nucleus in which the annihilation has occurred;
2. the energy loss by ionization in the ordinary matter of the two targets.

We shall discuss each step separately.

4.1. Hyperon-nucleon elastic scattering

We assume, on the basis of ref. [10], that the total elastic cross section for the $\Xi^- p$ and $\Xi^- n$ scattering processes be $\sigma_E \approx 10$ mb. Moreover, we assume a differential elastic cross section $d\sigma_E/d\Omega \propto \exp(B \cdot t)$, where t is the second Mandelstam variable, and B is suitably taken as 5 GeV^{-2} [11]. Furthermore, we model the nucleus as a homogeneous sphere of nucleons of radius $R_{\text{nuc}} = R_0 \cdot (A - 1)^{1/3}$ ($R_0 \approx 1.35$ fm).

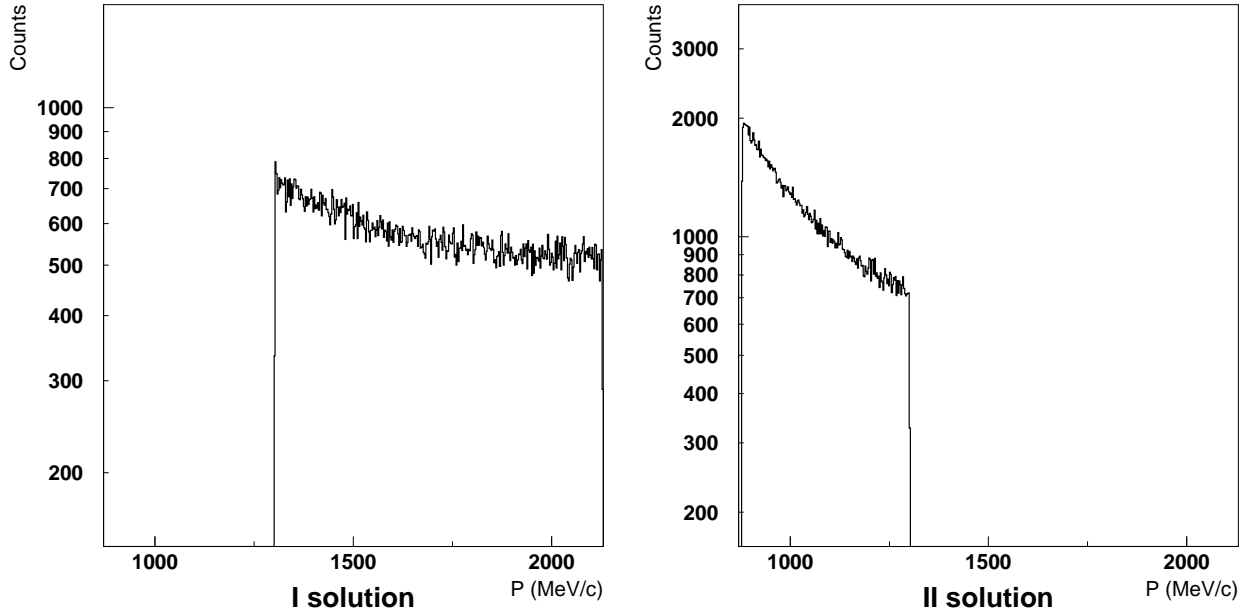


Figure 2: Simulated $P(\Xi^-)$ momentum spectrum after SCR, for both first and second kinematical solution. We assume an isotropic angular distribution in the centre of mass frame of reference.

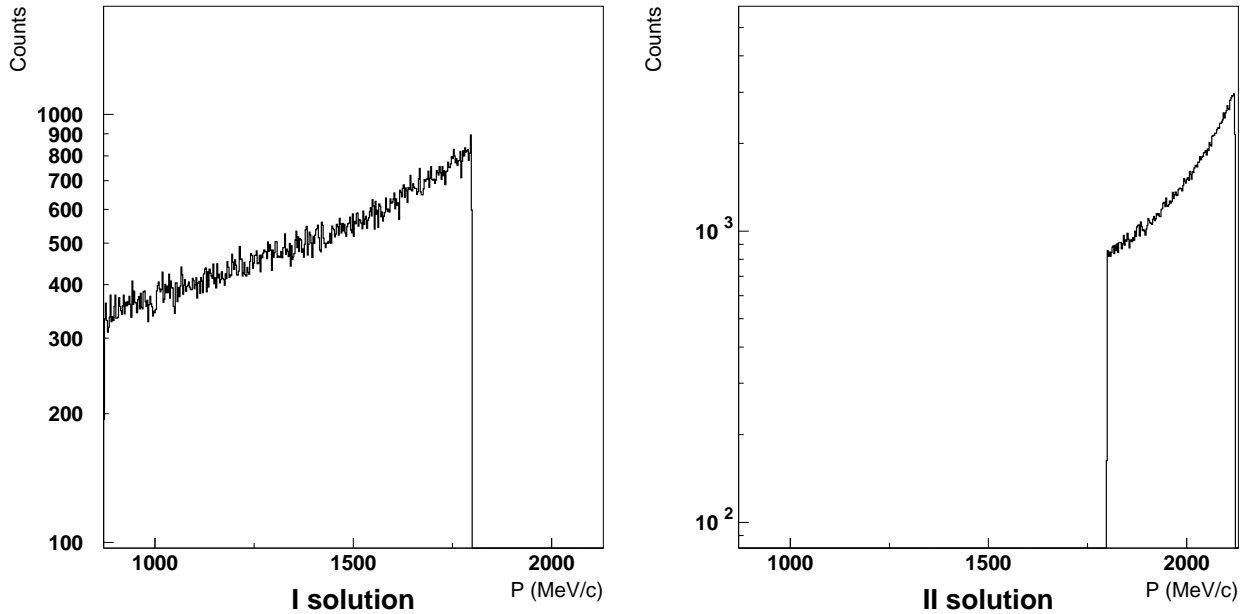


Figure 3: Simulated $P(\Xi^0)$ momentum spectrum after SCR, for both first and second kinematical solution.

We perform the numerical simulation of this first slowing down step in the framework of an INC-like (Intra Nuclear Cascade) model [12], starting from the distribution of fast hyperons shown in fig. 2. The basic hypothesis of this model is that the $(A - 1)$ residual nucleus does survive for a time longer than the time spent by

the hyperon during its intra-nuclear path. Furthermore, the scattering exit angle of Ξ^- after each nuclear scattering is chosen uniformly in the centre of mass frame of reference.

As far as nuclear scattering events are concerned, we treat these processes as instantaneous since the calcu-

lated average spent time is of order 10^{-22} s (proper time), while the Ξ^- mean life, in its rest frame of reference, is $\tau_{ML} = 1.639 \cdot 10^{-10}$ s.

We obtain that, from the $2 \cdot 10^5$ simulated random walks, 9.1% of the hyperons scatter in the residual nucleus at least once if we consider the first kinematical solution (the maximum number of consecutive scattering events being 3), and 31% considering the second solution (and the maximum number of scattering events is, correspondingly, 8).

The main physical effects due to hyperon-nucleon elastic scattering are twofold: on one hand, the $P(\Xi^-)$ momentum spectrum is modified with respect to that of fig. 2, showing a low momentum tail from 1301 MeV/c down to ~ 96.6 MeV/c (first solution) and from 877 MeV/c to ~ 18.7 MeV/c (second solution); on the other hand, the angle θ_{nuc} between the exit direction and the antiproton direction ($\theta_{\text{nuc}} \equiv \theta(\Xi^-)$ if the hyperon does not scatter at all), after the nuclear scattering process, spans from 0 up to 1.48 rad and 2.38 rad, respectively, which are much higher than the limit angle θ_{max} defined in sec. 3. Thus, this first step provides a non negligible fraction of hyperons with relatively low momentum and large angles. The next step, involving the passage of particles through matter and the ionization energy-loss, further modifies the momentum spectrum, without modifying the θ_{nuc} angle. Due to the low probability, the nuclear scattering of the hyperon inside the target has been neglected. Thus, the final flight in the experimental apparatus is a simple straight line.

4.2. Energy-loss by ionization

In the study of the energy-loss during the passage of particles through matter, the geometry of the experimental setup plays a crucial role, because it determines the effective hyperon path as a function of the exit angle θ_{nuc} , and thus the slowing down effectiveness.

We adopt here a simple geometry consisting of two distinct targets: the first one, in which the SCR takes place, is a thin parallelepipedal wire of Gallium or Gold (4 cm long and $5 \mu\text{m} \times 5 \mu\text{m}$ square) orthogonal to the beam direction, while the second one is a diamond parallelepiped (4 cm \times 4 cm as transverse dimensions and 2 cm thick) with a hole of radius 0.25 cm in its centre. The two targets are separated by a 1 mm vacuum gap.

The physics of our simulation essentially relies on the Bethe-Bloch equation, which expresses the mean rate of energy-loss per unit length: we take it from [13] and we report it here for the sake of discussion

$$-\frac{dE_K}{dx} = K\rho \frac{Z}{A} \frac{1}{\beta^2} \left[\frac{1}{2} \ln \left(\frac{2m_e c^2 \beta^2 \gamma^2 T_{\text{max}}}{I^2} \right) - \beta^2 - \frac{C}{Z} - \frac{\delta}{2} \right], \quad (7)$$

with

$$T_{\text{max}} \equiv \frac{2m_e c^2 \gamma^2 \beta^2}{1 + 2\gamma \frac{m_e}{M_0} + \left(\frac{m_e}{M_0} \right)^2}, \quad (8)$$

where E_K is the hyperon kinetic energy, ρ is the density of target material, $K = 0.3 \text{ MeV} \cdot \text{cm}^2$, Z and A are the atomic number and the mass number of medium, β is the dimensionless velocity of hyperons, m_e is the electron mass, $\gamma = (1 - \beta^2)^{-1/2}$ is the relativistic factor, I is the mean excitation energy, M_0 is the hyperon rest mass and c is the speed of light. The parameters C and δ , usually negligible at high energy, play an important role in our simulation because the final stage of the slowing down process takes a major fraction of the total time spent by the hyperon before being stopped; the value of δ has been taken from the accurate work of Sternheimer *et al.* [14] and reads

$$\delta = \begin{cases} 2X \ln 10 + C & X \geq X_1 \\ 2X \ln 10 + a(X_1 - X)^m + C & X_0 \leq X \leq X_1 \\ 0 & X \leq X_0 \end{cases}, \quad (9)$$

with $X = \ln \beta \gamma$, and where C , a , m , X_0 , X_1 are taken from ref. [14] for the diamond target.

The total time T elapsed during the energy-loss process is comparable with the Ξ^- mean life, τ_{ML} : thus, a fraction of hyperons decays prior to complete stopping.

In order to evaluate the number of surviving Ξ^- 's, the following procedure has been adopted. Each Ξ^- has been assigned a lifetime τ according to the $\exp(-\tau/\tau_{ML})$ distribution, in the frame in which the particle is at rest; at each interval of lost kinetic energy dE_K , the corresponding time interval dt (in the laboratory frame) spent by Ξ^- to travel a path dx has been transformed into the rest frame in order to obtain the total proper time elapsed T , and compare it with the proper lifetime τ . Thus, eq. 7 should be solved provided that the condition

$$T = \int_0^{t_F} dt \sqrt{1 - \beta^2} \leq \tau, \quad (10)$$

be satisfied, where t_F is the final time after complete stopping of the hyperon in the laboratory frame of reference.

Eq. 7 can be formally expressed through

$$\frac{dE_K}{dx} = -g(E_K). \quad (11)$$

Furthermore, the hyperon momentum P depends over E_K as

$$P(E_K) = \sqrt{E_K(E_K + 2M_0)}. \quad (12)$$

From eqs. 10, 11 and 12, we straightforwardly obtain

$$R = - \int_{E_K^{\text{in}}}^0 dE_K \frac{1}{g(E_K)}, \quad (13)$$

$$T = -\frac{M_0}{c} \int_{E_K^{\text{in}}}^0 dE_K \frac{1}{g(E_K)P(E_K)} \leq \tau, \quad (14)$$

where R is the stopping range and E_K^{in} is the hyperon's initial kinetic energy. Performing a numerical integration of eq. 13, at each step the corresponding time integral of eq. 14 is calculated and checked whether T is lower or greater than the lifetime τ . In the former case the integration proceeds until complete stopping, otherwise the hyperon decays along its path.

5. SIMULATION RESULTS

The simulation procedure described in the previous section has been applied to the above mentioned geometry (a wire as Ξ^- production target followed by a second one as hypernuclear target); furthermore we run the simulation twice, considering two different materials (gallium and gold) for the wire, in order to check the effectiveness of the atomic weight on hyperon production. For both materials, $2 \cdot 10^5$ Ξ^- 's have been generated in a spot of radius $r = 10 \mu\text{m}$ on the surface of the wire.

The calculated parameters of our simulation are:

- the fraction f_{stop} of hyperons stopped in the second target;
- the fraction f_{dec} of hyperons decayed before stopping;
- the fraction f_{loss} of hyperons lost in the gap between the two targets or in the central hole of the second target.

Since reaction 1 can produce Ξ^- 's of two different momenta, both kinematical solutions have been simulated separately.

The most relevant parameters for the experiment are the total number N_{stop} of stopped and detected Ξ^- 's per second and the number $N_{\Lambda\Lambda}$ of produced and detected double hypernuclei per second. In order to calculate these values from the simulated fractions already defined, one has to make a few reasonable assumptions about the luminosity of the machine and the detection efficiency; moreover, other physical parameters mentioned below have been roughly estimated just to get a first insight of the rates, though further accurate evaluation is needed.

As already discussed in sec. 3, we have assumed a total cross section $\sigma_{SCR} \approx 2 \mu\text{b}$ for the SCR reaction between an antiproton and a free nucleon at 3 GeV/c; accordingly, the corresponding reaction cross section of reaction 1 occurring on a neutron inside a nucleus reads

$$\Sigma_{SCR} \approx \sigma_{SCR} \cdot A^{2/3} \cdot \frac{A-Z}{A}, \quad (15)$$

Table I: Results of the Monte Carlo simulation of the double hypernuclei production, considering two materials (gallium and gold) for the hyperon production wire. Each kinematical solution has been investigated separately, and the corresponding results are shown. (See text for the physical meaning of the different parameters).

	Gallium wire		Gold wire	
	I	II	I	II
f_{stop}	$5.75 \cdot 10^{-4}$	$1.15 \cdot 10^{-2}$	$1.45 \cdot 10^{-3}$	$2.01 \cdot 10^{-2}$
f_{dec}	$7.98 \cdot 10^{-2}$	$1.31 \cdot 10^{-1}$	$8.72 \cdot 10^{-2}$	$1.47 \cdot 10^{-1}$
f_{loss}	$3.76 \cdot 10^{-2}$	$4.44 \cdot 10^{-2}$	$3.73 \cdot 10^{-2}$	$4.39 \cdot 10^{-2}$
$N_{\text{stop}} [\text{s}^{-1}]$	0.460	9.224	1.16	16.07
$N_{\Lambda\Lambda} [\text{s}^{-1}]$	$1.15 \cdot 10^{-4}$	$2.31 \cdot 10^{-3}$	$2.90 \cdot 10^{-4}$	$4.01 \cdot 10^{-3}$

where the surface annihilation scaling has been taken into account [15].

Furthermore, we assume a luminosity of the antiproton beam of roughly $\mathcal{L} \approx 10^{32} \text{cm}^{-2}\text{s}^{-1}$, as realistically expected at HESR, and a reconstruction efficiency for the whole detector $\varepsilon_K \approx 0.5$.

Following refs. [11, 16], we also assume that the conversion probability (i.e. the probability for the hyperonic Ξ^- -nucleus conversion into a $\Lambda\Lambda$ -hypernucleus) per stopped Ξ^- be $p_{\Lambda\Lambda} \approx 0.05$, and that the level population fraction be $p_{LP} \approx 0.1$; the probability of transition per event has been taken as $p_T \approx 0.5$ and the γ -photo peak efficiency as $\varepsilon_\gamma \approx 0.1$.

Thus, the number of stopped Ξ^- 's and of formed $\Lambda\Lambda$ -hypernuclei can be calculated through

$$N_{\text{stop}} = \mathcal{L} \cdot \Sigma_{SCR} \cdot f_{\text{stop}} \cdot \varepsilon_K, \quad (16)$$

and

$$N_{\Lambda\Lambda} = N_{\text{stop}} \cdot p_{\Lambda\Lambda} \cdot p_T \cdot p_{LP} \cdot \varepsilon_\gamma. \quad (17)$$

The final results are reported in tab. I for both gallium and gold wires and both kinematical solutions.

The relative weight of each solution is at present totally unknown as no measurements of the differential cross section for reactions 5 and 6 exist nor theoretical estimates as well. Hence, the actual value of $N_{\Lambda\Lambda}$ is located between the two values of first and second solution reported in tab. I. Being conservative, one may take the value of the first solution only; nevertheless, even in this pessimistic hypothesis, the total number of stopped Ξ^- 's is around $1.19 \cdot 10^6$ per month and the total number of formed double hypernuclei is around 300 per month considering the gallium wire, while we obtain $3 \cdot 10^6$ and 750 respectively when considering the gold wire.

On the other hand, if the \bar{p} annihilation occurs through reaction 2 instead of reaction 1, the processes of Ξ^- slowing down and double hypernuclei formation are in practice identical to those considered so far: therefore, it is

reasonable to expect that the total Ξ^- production and double hypernuclei formation should be enhanced by a factor $A/(A-Z) \sim 1.8$.

As a first indication from the values of the stopped Ξ^- 's, one can observe that the weight of the nucleus strongly influence the hyperon slowing down through nuclear scatterings.

Of course these results depends on the estimates of the machine, detector and physical parameters chosen for our simulation, but the values assumed here seem quite realistic indeed. In fact, HESR design's first priority is the high luminosity and the PANDA apparatus will be an ensemble of several detectors with good reconstruction capabilities.

6. CONCLUSIONS

A preliminary evaluation of the rates for the complete stopping of a Ξ^- hyperon, produced through a high energy antiproton interacting with a gallium or a gold nucleus, in a diamond (carbon) target has been performed using a Monte Carlo technique based on an INC-like model. The chosen geometry is suitable for the PANDA experiment project at the future HESR machine at GSI.

The results, relying on the expected performances of the apparatus, show the feasibility of a large production of double hypernuclei: our preliminary estimates, in terms of stopped Ξ^- 's and formed double hypernuclei, are larger than the previous data existing in literature and also larger than the expectation of other future experiments and machines.

A lot of calculations are of course still necessary in order to fully design the geometrical arrangement, the sizes and the materials of the targets, in order to optimize the production and to meet the beam requirement of the

machine, and this will be the future work for the next months.

-
- [1] M. Danysz *et al.*, Nucl. Phys. **49**, 121 (1963).
 - [2] D. Prowse *et al.*, Phys. Rev. Lett. **17**, 782 (1966).
 - [3] R. L. Jaffe, Phys. Rev. Lett. **38**, 195 (1977); Phys. Rev. Lett. **38**, 617(E) (1977).
 - [4] J. Pochodzalla, Nucl. Instr. and Meth. in Phys. Research B **214**, 149 (2004) (and references therein).
 - [5] K. Kilian, *Physics at LEAR*, Eds. C. Amsler *et al.*, Harwood Academic Publishers, 1988.
 - [6] J. K. Ahn *et al.*, in: Proc. of the First International Symposium on Hadrons and Nuclei, Edited by Il-T. Cheon *et al.*, 2001 AIP, p. 180-188.
 - [7] S. Aoki *et al.*, Prog. Theor. Phys. **85**, 951 (1991); A. Ichikawa *et al.*, Phys. Lett. B **500**, 37 (2001).
 - [8] S. Aoki *et al.*, Prog. Theor. Phys. **85**, 1287 (1991).
 - [9] A. B. Kaidalov and P. E. Volkovitsky, in: Agenda of the 2nd Meeting of the Working Group: Physics with Secondary Beams, GSI (1996).
 - [10] G. R. Charlton *et al.*, Phys. Lett. B **32**, 720 (1970); R. A. Muller, Phys. Lett. B **39**, 671 (1972); J. M. Hauptman *et al.*, Nucl. Phys. B **125**, 29 (1977)
 - [11] J. Pochodzalla *et al.*, private communication, 2003.
 - [12] M. Cahay, J. Cugnon and J. Vandermeulen, Nucl. Phys. A **393**, 237 (1983) (and references therein).
 - [13] Review of Particle Physics, Phys. Rev. D **66**, (2002).
 - [14] R. M. Sternheimer, M. J. Berger and S. M. Seltzer, Atomic Data and Nuclear Data Tables **30**, 261(1984).
 - [15] F. Iazzi, in: Proceedings of the First International Symposium on Hadron and Nuclei, Edited by Il-T. Cheon *et al.*, 2001 AIP, p. 21-27; M. Astrua *et al.*, Nucl. Phys. A **697**, 209 (2002).
 - [16] T. Yamada and K. Ikeda, Nucl. Phys. A **585**, 79c (1995); T. Yamada and K. Ikeda, Phys. Rev. C **56**, 3216 (1997); Y. Hirata *et al.*, nucl-th/9711063.